Characterisation of short-length scale residual stress variations within an electron beam welded P91 Ferritic–Martensitic steel plate

Journal Item

Research article

Characterisation of short-length scale residual stress variations within an electron beam welded P91 Ferritic–Martensitic steel plate

N. Naveed [a,b,*]

[a] Faculty of Technology, University of Sunderland, Sunderland, SR6 0DD, UK
[b] The Open University, Walton Hall, Milton Keynes, MK7 6AA, UK

ABSTRACT

In this research, an electron beam (EB) butt-welded P91 steel plate (~9 mm thick) is selected to measure longitudinal residual stresses (acting in the welding direction) using a promising residual stress measurement technique - the contour method. The EB weld causes short length scale residual stresses within the narrow width of the fusion zone with steep stress gradients lateral to the weld line, which presents a new challenge for the residual stress measurements. The special measures were taken for all main steps of the technique to improve its the spatial resolution, thereby the short length scale residual stresses were captured. The success of the measurement is assessed by comparing the contour method result to the neutron diffraction result, and a good agreement were found in the results of both the techniques. These results also shows that the contour measurement results successfully captured the steep stress gradient on both sides of the weld centre-line (0 mm) with tensile stress peaks situated just 2.8 mm apart. It is one of the best resolutions in residual stress length-scale in this component achieved in contour measurements.

1. Introduction

Ferritic martensitic steels are increasingly used in manufacturing of high integrity structural components such as main steam pipes, boilers, steam headers, turbine castings and super heater tubings of ultra-supercritical power plants and fossil fuelled power generating plants that sustain elevated temperatures [1, 2]. Ferritic martensitic steels containing 9–12 wt. % chromium offer a better high temperature creep resistance than the classical 2.25 Cr–1Mo grades. They are less susceptible to degradation through thermal fatigue due to having a lower coefficient of thermal expansion and higher thermal conductivity compared with stainless steel [3, 4]. However, P91 weldments (made by conventional welding process) in service operation can exhibit premature failure due the high tensile residual stress distribution along the welded joint. The failure type falls into the category of 'type IV' cracking due to the position of the cracks. In this case, the weldments will be weakest due to formation of creep voids in the refined (inter-critical) region of the HAZ of the weld [3, 5]. The tensile properties and hardness of P91 weldments can also be improved by using the normalizing treatment. However, to improve long term creep properties, the earlier grades of 'type 91' steels are modified through small additions of niobium (Nb), vanadium (V) and nitrogen (N)

[6, 7]. The modified P91 steels are used together with high energy electron beam welds to enhance the resistance to type IV cracking [8].

High energy density welding (HEDW) processes such as electron beam welding (EB) are capable of providing high penetration into a component [9]. Autogenous EB welds produce excellent joint fits without introducing excessive heat and distortion. They have a deep, narrow and parallel sided fusion zone in the vicinity of the weld, due to the small thermal contraction in the weld metal compared to conventional welding processes such as arc welding [10, 11]. The small thermal contraction prevents excessive angular deformation, bowing, buckling and twisting of the component. High energy electron beam welds are less prone to type IV cracking and likewise less premature failure. However, there are some disadvantages of the EB welding process. Because of the very high cooling rate, the molten material formed in the welding process rapidly solidifies and shrinks. This can cause many unwanted consequences such as material property changes, cracking within the weld, changes of shape and deformation in some materials, for example high carbon steel [12]. Furthermore, the EB welding process produces a significant level of residual stresses in the direction of the weld (longitudinal direction). The magnitude of these stresses are considerable at the weld centre line and form a very fine steep gradient moving away from the weld line within a

small region [13, 14]. Therefore, it is of paramount importance that the initial state of residual stress is well characterised. This will provide an important base to recognise the behaviour of engineering components when they are in used during service loading.

High stress gradients over very short distances associated with EB weld type becomes it necessary to make stress measurements on as small and highly precise region as possible. Thus, measurement spatial resolution is an important consideration for residual stress investigation of this welded components. The limitations of the deep-hole drilling (DHD) technique have been studied previously, observed it less suited to resolving short length scale residual stress variations in thin section EB welds. A thick cylindrical steel EB welded sample has been tested using the DHD drilling method [15]. But the spatial resolution of the residual stress measurement was limited by the 5 mm diameter trepanned core. It can also be affected by stress relaxation due to progression of plastic unloading during trepanning the material [16]. Recently, some advancement has been proposed in this technique to measure the through-thickness residual stress distribution with a comparatively lower degree of damage to the specimen. However, the application of this need to be explored in the thin welded components [17]. The neutron diffraction measurement technique has sufficient spatial resolution and depth penetration for many cases. However, the application of this technique has some additional limitations: for example it is not suitable for near surface measurements [18], it is sensitive to the material grain size and texture, and it can be difficult to obtain reliable stress free lattice parameter measurements [19]. In addition to this, for the thick components (>40 mm), the neutron diffraction technique is not worked well for measuring residual stresses. Residual stress measurement results for an EB welded plate using neutron diffraction have been reported in [14, 20]. However, reliable stress measurements were not achieved within and around the weld region because of variations in reference lattice constant measurements.

The contour method has emerged as a promising technique for the measurement of residual stresses in engineering components. This method was invented in 2000 by Mike Prime [21]. It is based on cutting the test component of interest in two halves. The cut surfaces deform, owing to the relaxation of residual stresses. The deformations of the two cut surfaces are then measured, and used to back calculate the 2-dimensional map of original residual stresses normal to the plane of the cut [22]. The contour method is effective of measuring through-thickness stresses. This technique is relatively simple, inexpensive, and utilizes readily available equipment in workshops [23]. It has been successfully validated by commonly used residual stress measurement techniques, such as neutron diffraction [24], slitting [25, 26], synchrotron x-ray diffraction [27, 28] and sectioning [29]. The method is useful to obtain detailed information of residual stresses introduced by various manufacturing processes such as welding [23, 30, 31, 32], hammer peening [33], laser peening [34, 35, 36], cold expanded hole [37] and aluminium alloy forging [38]. Nevertheless, like the other residual stress measuring techniques, the contour method also suffers from factors that impact on the accuracy and the spatial resolution of the method, and cause uncertainties in the measured stresses. The residual stress measurement results for a EB welded plate using the contour method have been reported in [38]. However, reliable stress results were not achieved within and around the weld region because of the limited spatial resolution of the method. The reliability and accuracy of the contour method measurement results can be improved by minimising errors and uncertainties that can be introduced during cutting and data analysis procedures. In another study, the residual stress was investigated in

electron-beam welded Ti–6Al–4V alloy rings using different measurement techniques including X-ray diffraction (XRD), hole drilling method and the contour method, and there is a good correlation found in the residual stress results [40]. However, in this study it was not demonstrated that how the contour method steps were implemented such as specimen cutting to avoid cutting artefacts and selection of appropriate parameters such as surface deformation measurement spacing, data smoothing parameters ('knot spacing' for example cubic spline smoothing) and finite element mesh size. All steps in the contour method [21, 41] contribute some errors and uncertainty in the measured stresses. In order to achieve high-precision measurements, appropriate knowledge to perform each step has to be acquired. Previously, errors related to the cutting step that are dependent on stress magnitude, such as bulge error [42] and plasticity error [43], have been addressed. Other limited studies address errors related to the cutting step that are independent of the stress magnitude where cutting artefacts are present in the surface contour data [30, 44, 45]. In order to minimise the error related to the cutting process, cutting conditions can be optimised by performing trial cuts on a stress free part of the test component [45, 46, 47], or on another piece of similar stress free material [42].

The contour method steps should perform in a manner that they do not change the underlying features of surface deformation especially where the residual stress distribution varies over short distances such as EB welded components. Therefore, to carefully implement these steps, it is important to select appropriate parameters such as surface deformation measurement spacing, data smoothing parameters ('knot spacing' for example cubic spline smoothing) and finite element mesh size. Recently, the research has been done to investigate these important parameters [48]. In this research, a simple approach for choosing initial parameters is developed based on an idealised cosine displacement function (giving a self-equilibrated one-dimensional residual stress profile). In that research, guidelines are proposed to help the measurer to select the most suitable choice of these parameters based on the estimated wavelength of the residual stress field. In this paper, these guidelines are considered to select deformation measurement spacing and data analysis parameters for improving the spatial resolution of contour measurements. For this study, an electron beam (EB) butt-welded P91 steel plate (~9 mm thick) was used to measure longitudinal residual stresses (acting in the welding direction) using the contour method. The EB weld causes short length scale residual stresses within the narrow width of the fusion zone with steep stress gradients lateral to the weld line. In order to capture the short length scale residual stresses, the special measures are taken for all main four steps of the technique. The success of the improvements implemented is assessed by comparing the new measurements with conventional contour method results and published neutron diffraction results.

2. Materials and methods

2.1. Specimen detail

The chemical composition for the base material of the EB welded P91 steel plate used for the present investigation is given in Table 1 [39]. The test specimen was fabricated from a hot rolled plate material. As a first step of specimen preparation, the hot rolled plate material was normalized at 1050 °C for 1 min mm^{-1} thickness. Then, it was tempered at 770 °C for 3 min mm^{-1} followed by cooling in air. Then, the tempered material was machined to create plates of dimensions 290 mm long by 75

Table 1. The chemical composition of the Mod.9Cr–1Mo steel (remaining Fe) [39].

C	Mn	Zr	Si	P	S	Cr	Mo
0.106	0.443	0.005	0.221	0.018	0.0008	8.965	0.901
Ni	Cu	Al	N	Nb	Ti	V	
0.212	0.045	0.010	0.0464	0.073	0.004	0.194	

Table 2. The welding parameters for the EB welded P91 steel plate [39, 50].

Welding parameters	
Beam current (mA)	70
Gun voltage (kV)	60
Travel speed (m/min)	1
Pre-heat (°C)	No

mm wide by 10 mm thick. Finally, the top and bottom surfaces of the sample plates were ground to get flat parallel surfaces by removing the surface irregularities caused by the hot rolling fabrication process. A final plate thickness of ~9 mm was achieved [39]. Pairs of prepared plates were then butt welded along the 290 mm edge by an electron beam process. The recorded welding parameters are given in Table 2. The final dimensions of the test plate obtained were 290 mm length, 150 mm width and ~9 mm thick. In this study, the plate is used for residual stress measurement in the as-welded state. The contour residual stresses are analysed using a bulk Young's modulus of 218 GPa and a Poisson's ratio of 0.3 for both the P91 base metal and the fusion zone.

2.2. First contour measurement

The first contour residual stress measurement was carried out using a conventional contour method [39]. The longitudinal residual stress was determined by performing the contour cut across the mid-length of the plate, in the normal direction to the weld as shown in Figure 1. Before specimen cutting, sacrificial layers were attached along the plane of the cut to both faces (top and bottom) of the plate. They help to avoid undesirable wire entry and exit effects [45]. These were made up of carbon steel with a 5 mm × 10 mm cross-section. In order performed a precise cut, an Wire Electro Discharge Machine (EDM) was employed. The cut was performed using a 0.25 mm diameter brass wire. This diameter of wire provides limited surface finish and which will restrict the stress resolution length-scale. After finishing the cut, a Mitutoyo Crysta Plus 547 CMM with 4 mm diameter Renishaw PH10M touch trigger probe was used to measure the deformation of the contour cut surfaces by using 0.5 mm measuring density. The contour cut surface data were prepare into a suitable form using standard contour routines coded in MATLAB 7.10. The cut surface data was processed using basic steps such as alignment of the two data sets, removing of noise and outliers in the raw data, averaging of the measurements points from the pair of cut halves and smoothing by fitting cubic spline functions, with a 1 mm × 1 mm knot spacing [39]. The data analysis steps are discussed in detail in [50, 51]. Finally, the linear elastic finite element analysis was carried out using ABAQUS. For the 3D model, one half of the plate was built in the software by extruding the measured shape of the perimeter at the cut interface. The contour cut surface was modelled as a flat surface because the displacements values that were measured from the contour cut surfaces
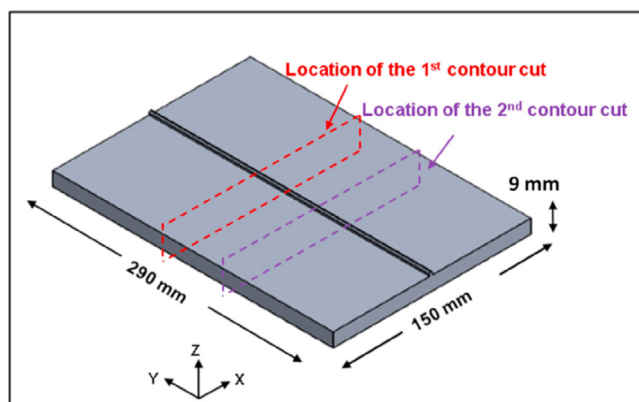
were very small and the analysis is elastic. The cut face was meshed using 0.5 mm size first order elements. The processed surface contour data were applied as boundary conditions, with reverse sign at the cut face nodes of the FE model. The elastic material properties (Young's modulus, E = 218 GPa and Poisson's ratio, $\vartheta = 0.3$) of the specimen were defined and the elastic FE analysis conducted to determine the released residual stress distribution across the created cut surface. The longitudinal residual stresses map from the first cut measured using the conventional contour method [39] is represented in Figure 2. The conventional contour stress results are compared with published neutron diffraction measurements [39, 49] along a line 1.5 mm below the top surface of the plate in Figure 3. The conventional contour measurement was conducted at the same mid-length location as the neutron diffraction measurements. For Neutron diffraction measurements, the gauge size of $(1 \times 1 \times 1)$ mm^3 are used for strains measured in the longitudinal direction. The longitudinal residual stress profile measured by neutron diffraction had an 'M' shaped stress distribution across the weld centre line. In these results, high tensile stress peaks were observed on both sides of the weld centre line beyond the heat affected zone (HAZ)/parent material boundary. The tensile peaks of this stress distribution are spread across a very short length, that is within ~3 mm spanning a 1 mm wide fusion zone. Overall, the residual stress results measured from both the methods show the same M-shaped trend. However, the contour method measurement has not captured the maximum tensile stress peaks on both sides of the weld centre line observed in the neutron diffraction results [39, 49]. This evidence illustrates the limited spatial resolution of the contour method measurement approach used.

Table 3 summarises the cutting conditions, deformation collection and data analysis parameters used for this "conventional" contour measurement and compares them with the guidelines presented in [48]. Note that the minimum residual stress wavelength, *w*, of interest is defined here based upon a residual stress wavelength estimated from the neutron diffraction measurements conducted on the same plate [39, 49].

2.3. Second contour measurement

A second contour cut was conducted with the aim to improve the spatial resolution of the contour method. The location of the second contour cut in one of the half-plates remaining from the first cut (145 mm long and 150 mm wide) is indicated in Figure 1. The second cut was made 60 mm away from the first contour cut plane as shown in Figure 4. The following sub-sections describe the details of the special measures taken in the cutting and data analysis steps to improve the quality of the contour measurement results.

2.3.1. Wire EDM cutting

Sacrificial layers 5 mm thick were attached on the top and bottom faces of the plate along the plane of the cut to avoid wire entry and exit artefacts [45]. A 1.8 mm diameter start pilot hole was drilled at 10 mm from one end of the plate. This provided an embedded cutting configuration giving self-restraint during cutting [43]. Finger clamping tools were used to provide support and to stop any movement of the test component on the EDM bed table. The test component and the fixture were left to reach thermal equilibrium conditions within the EDM deionised water tank before clamping to prevent any thermal stresses. It also helps to produce the cut surface with better precision and fine surface finish by minimising any recast layer and cutting induced stresses [30]. WEDM was used to carried out the cut. In order to improve the cut surface finish quality, the WEDM wire diameter was reduced for the second cut from 0.25 mm to 0.1 mm [42]. The set of WEDM cutting parameters were selected as a result of the study of cutting trials to optimise the WEDM cutting parameters. The cut was performed using the S3 (designated on the machine) set of cutting parameters with the 'A' (Pulse rise time) value of 0.2 μs and 'TAC' (Reduced pulse rise time A for difficult cutting conditions) value of 0.1 μs. After cutting, the cut length was reduced by 20 mm from both sides in order to remove cut start and stop effects.
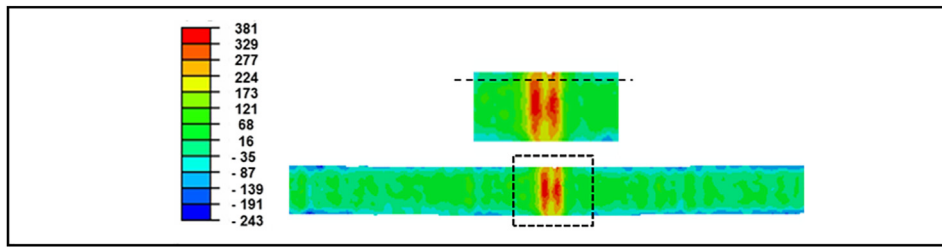

Figure 1. Sketch of the EB-welded P91 plate showing the locations of the contour cuts.

Figure 2. Map of the longitudinal stress measured using the conventional contour method [39]. Units are in MPa.
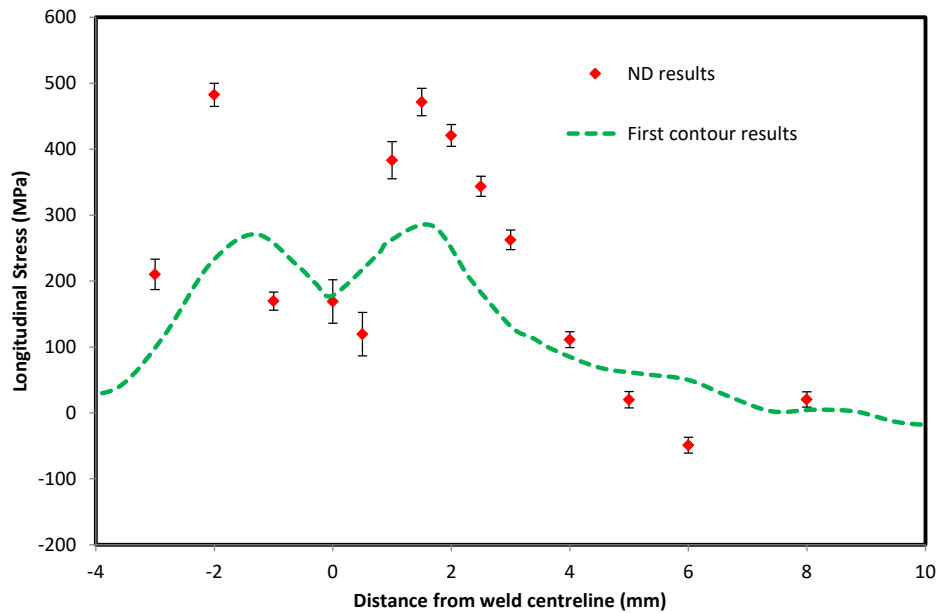

Figure 3. Comparison of the conventional contour method measurement with neutron diffraction measurements [39, 49] for a line profile at 1.5 mm below the top surface of the EB butt-welded P91 plate.

Figure 5 shows the different stages of the contour method. Figure 6 shows the contour cut surfaces after the cut.

2.3.2. Surface contour measurement

The thin cutting wire diameter (0.1 mm compared with 0.25 mm diameter for the first contour cut) produced a finer surface finish. Two further measures were taken to help improve the resolution of the short length-scale residual stresses in the plate. A 1 mm diameter Renishaw PH10M touch trigger probe (i.e. smaller than the 4 mm diameter probe used for the first cut) was used to measure the surface profiles of the cut parts in the Coordinate Measuring Machine - CMM (a Mitutoyo Crysta Plus 547) as shown in Figure 5 (c). Also, the measurement spacing was reduced from 0.5 mm to 0.125 mm.

2.3.3. Data processing and FE simulation

The surface deformation data from the second contour cut were processed using standard contour routines coded in MATLAB 7.10. as described in [50, 51]. Figure 7 shows the map of the averaged surface displacement measurements across the transverse cut plane. The maximum peak to valley deformation is about 32 μm in the region of the weld. Then, a cubic spline function was used with appropriate knot spacing to smooth the measured contour data. The criteria given in [48] were applied to make the best choices for suitable knot spacing (k) and finite element mesh size (s), based upon a residual stress wavelength (w) estimated from the neutron diffraction measurements and the hardness profile across the weld joint conducted on the same plate [39, 49]. Taking the minimum wavelength as $w = 3$ mm, an initial knot spacing $k \leq w/4$, that is $k \leq 0.75$ mm, should be selected and the finite element mesh size $s \leq w/12$, that is $s \leq 0.25$ mm, should be chosen. Then, the knot spacing was optimised using the uncertainty approach of Prime [50], by examining spacings ranging from 1 mm to 0.3 mm with 0.1 mm increments. Stresses were calculated for each k value using finite element analysis. A 0.25 mm mesh size was used for the cut face and adjacent to the cut face. The knot spacing was selected which minimised uncertainty in the calculated stresses [50]. Figure 8 illustrates that the minimum averaged stress uncertainty in the calculated stresses was found to be 17 MPa at a

Table 3. Cutting conditions, deformation collection and data analysis parameters for the first "conventional" contour measurement.

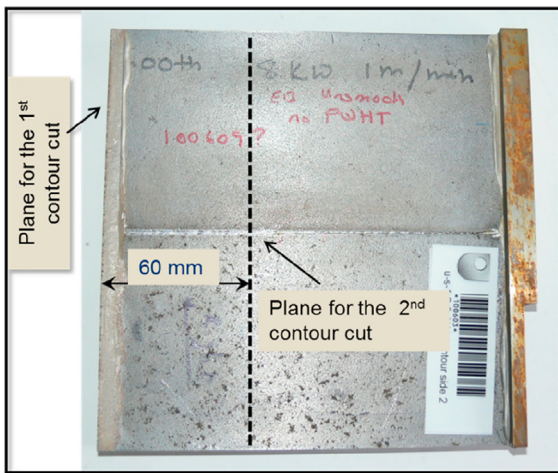| Case	Cutting wire Diameter (mm)	Deformation spacing, d (mm)	Knot spacing, k (mm)	FE mesh size, s (mm)	Residual stress wavelength, w (mm)
Conventional	0.25	0.5	1.0	0.5	3
Criteria	0.25	$<< k, \leq w/12$	$\leq w/4$	$\geq d, \leq w/12$	w
Met	Yes	No	No	No	-
Required	0.25	$<< 0.75, \leq 0.25$	≤ 0.75	≤ 0.25	3

Figure 4. Photo of one half of the EB welded P91 plate after the 1st contour measurement showing the location of the 2nd contour measurement cut.

knot spacing of 0.4 mm. Thus, a knot spacing of 0.4 mm was selected to smooth the surface deformation data. The processed contour data were then used to perform a final linear elastic finite element with the 0.25 mm mesh size. The elastic constants used in the analysis were a Young's modulus of 218 GPa and Poisson ratio 0.3. A map of the longitudinal residual stress measured using the improved contour approach is presented in Figure 9. The new results are compared with results from the first conventional contour measurement and the neutron diffraction measurements along a line 1.5 mm below the top surface of the plate in Figure 10. The macrostructure of the weld joint of the same EB welded plate has been examined previously [39] and showed the full penetration of the weld. It also showed that the width of the fused zone tapers from ~2.5 mm at the top of the plate and ~0.8 mm at the bottom. The width of the HAZ can also been seen to extend 0.8 mm beyond the fusion boundaries on both sides. The same macrograph was superimposed on to the stress map measured using the improved contour approach in Figure 9.

2.4. 3D surface roughness measurement

The surface texture and surface roughness over the first and second contour cuts were measured to investigate the quality of the cut surfaces using a confocal microscope with 10x magnification. The instrumental configurations for the confocal microscope are given in Table 4. The survey area was measured over a 15 mm region across the EB weld covering the whole thickness of the plate for both first and second cuts, as shown in Figure 11. A lateral spatial resolution of 12 µm was achieved by stitching data sets together. For the first cut, a S_q (the root-mean square) value of 2.9 µm and S_a (the arithmetic mean of the absolute height) value of 2.2 µm were measured. For the second cut a S_q value of 2.3 µm and S_a value of 1.8 µm were measured. Thus, the quality (roughness) of the second contour cut surface was improved by using a thinner wire diameter.
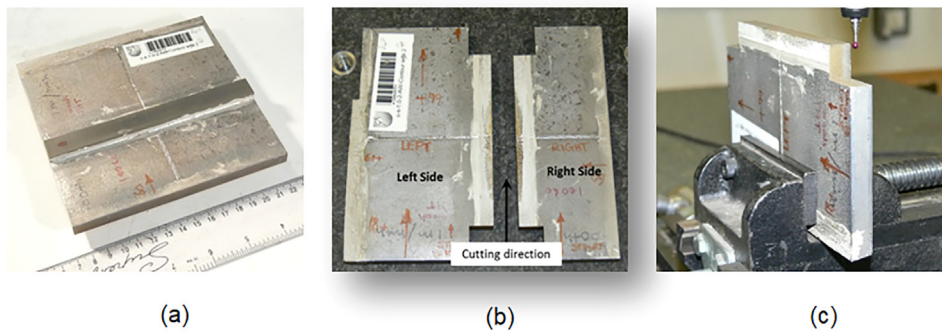

Figure 5. Represents different stages of the conotur method: (a) P91 plate with top sacrificial layer (b) Both parts of the plate after the second contour cut and removal of 20 mm from the wire cut start and stop edges (c) Measurement of surface profiles of the cut part using CMM with 1 mm diameter touch trigger probe.
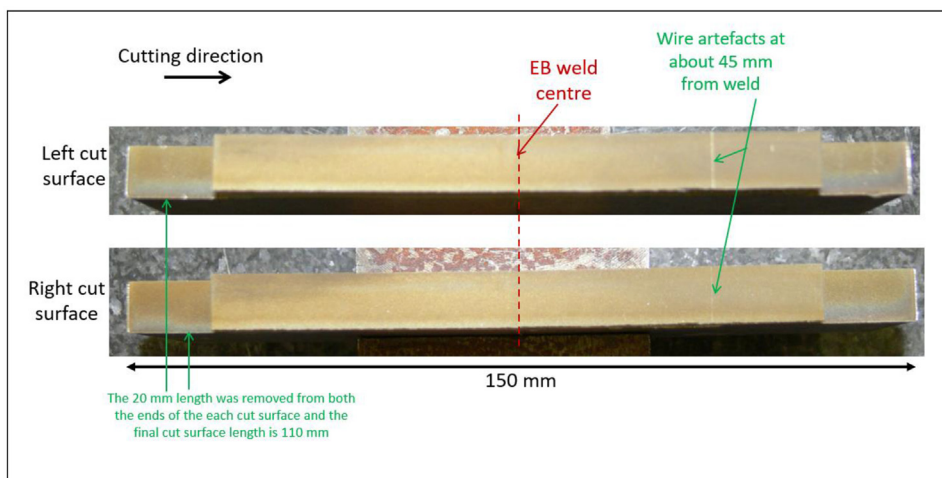

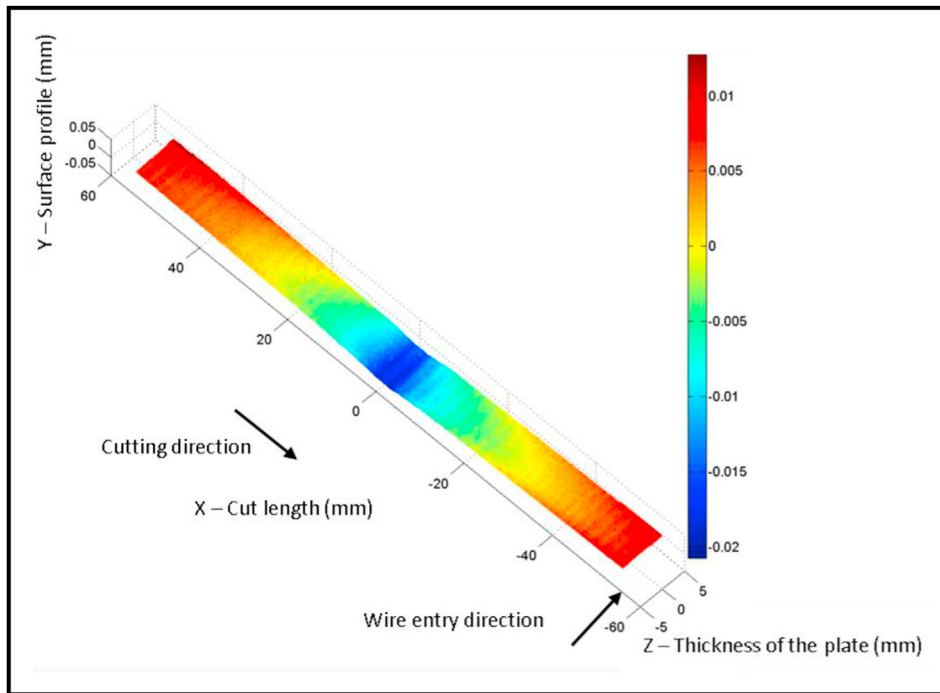**Figure 6.** Shows the contour cut surfaces with cutting details.

Figure 7. Map of averaged surface displacement measurements across the transverse cut plane (2nd contour cut) for the EB welded P91 steel plate (scale is mm).

3. Results and discussion for the EB welded P91 plate

An electron beam welded joint forms a narrow weld fusion zone that introduces short length scale residual stresses. For the EB welded P91 plate additional local stress variations arising from martensitic phase transformation were seen in neutron diffraction measurements [39, 49]. But the initial conventional contour method measurement was unable to resolve the tensile stress peaks in the HAZs adjacent to the weld fusion zone. The second contour cut used a smaller diameter wire to achieve a better surface roughness and implemented the criteria developed in [48] as summarised in Table 5 below. A knot spacing of 0.4 mm (smaller than $w/4$) was adopted on the basis of the uncertainties analysis described

earlier (see Figure 8). Sensitivity studies were carried for mesh size 0.25 mm and the effect of different knot spacings was observed. It can be seen that in Figure 12 that the large knot spacing failed to capture the dip in stresses at the weld centre arising from martensitic phase transformation. On the other hand, the small knot spacings more precisely captured the stress distribution at and around the weld region.

A map of the longitudinal residual stress measured using the improved contour approach is presented in Figure 9. The overall distribution suggests low stresses near to the weld within the HAZ and in the weld bead, and regions of high tensile stress at both sides of the weld in the parent material. Figure 10 shows comparison of the second and first contour measurements with neutron diffraction measurements [39,49]
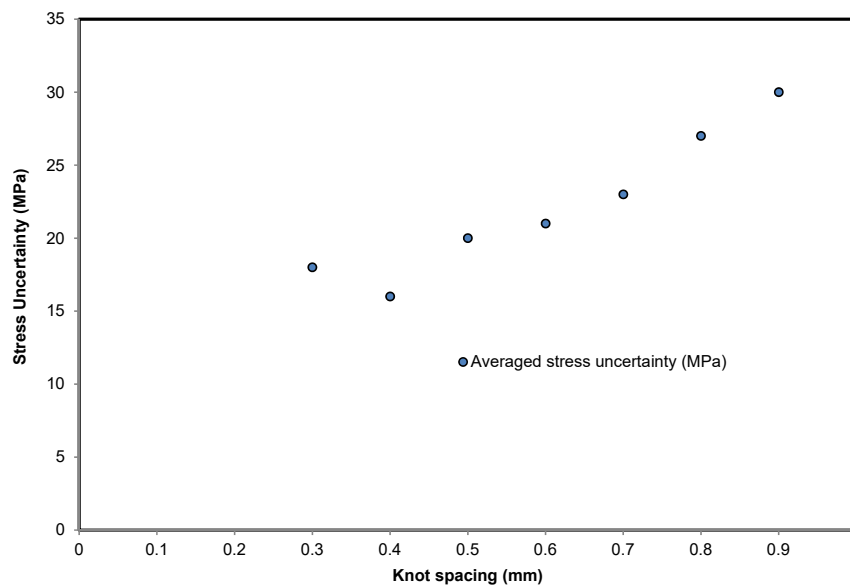

Figure 8. Optimal knot spacing indicated by minimising the averaged uncertainty in calculated stresses for the 2nd contour measurement of the EB P91 butt-welded plate.
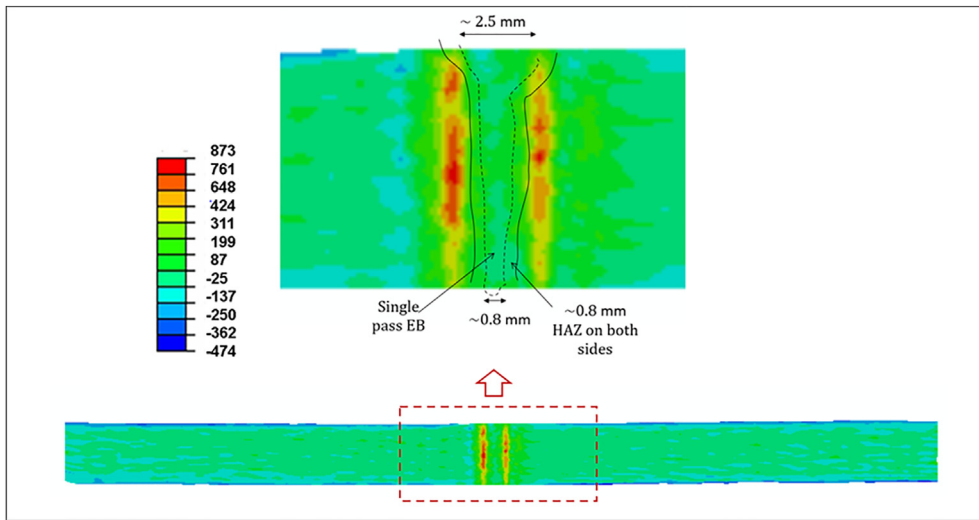
Figure 9. Map of the longitudinal stresses from the improved (2nd cut) contour measurement. (Units are in MPa).
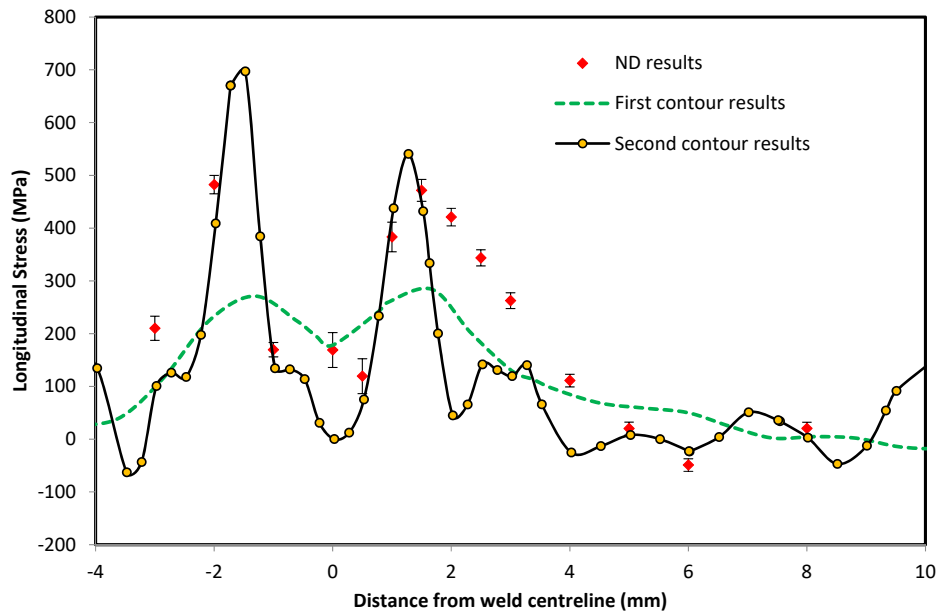

Figure 10. Comparison of the improved and original contour measurements with neutron diffraction measurements [39,49] for a line profile at 1.5 mm below the top surface of the EB butt-welded P91 plate.

for a line profile at 1.5 mm below the top surface of the plate. It shows that in the second contour results, the tensile stress peaks and approaching steep gradients have been successfully captured on both sides of the weld centre line. The contour method tensile stress peaks are situated 2.8 mm apart. Sharp stress variations are also found in the contour results away from the peak tensile stress region. This is most likely to be because of over fitting of the surface displacement data away from the weld region. This problem can be resolved by controlling the knot spacing along the cut length. Finer knot spacing can be used for a highly concentrated stress region with a short residual stress length-scale

and for the rest of the cut length relatively coarser knot spacing can be used where the wavelength of this stress field is much larger. There are low stresses found in the weld bead and stresses rise sharply to around 697 MPa and 540 MPa on right and left sides of the weld as shown in Figure 10. The asymmetric shape of the residual stress profile found cross the distance from weld center-line that might be because of the plastic deformation occurred during cutting process [52], despite the special measures were taken to minimise this effect (the cut was started from a small pilot hole and embedded cutting configuration was used to self-restraint the specimen during the cutting). These results can be further improved by further investigating the cutting direction and claiming configurations to reduce the plastic deformation and the stresses associated with it [53]. The new contour stress results within the weld region and HAZ are closely aligned with the neutron diffraction results as shown in Figure 10 along the line 1.5 mm below the top surface, except at the weld centre where the contour measurement indicates a dip to zero stress. This reduction is plausible owing to martensitic solid
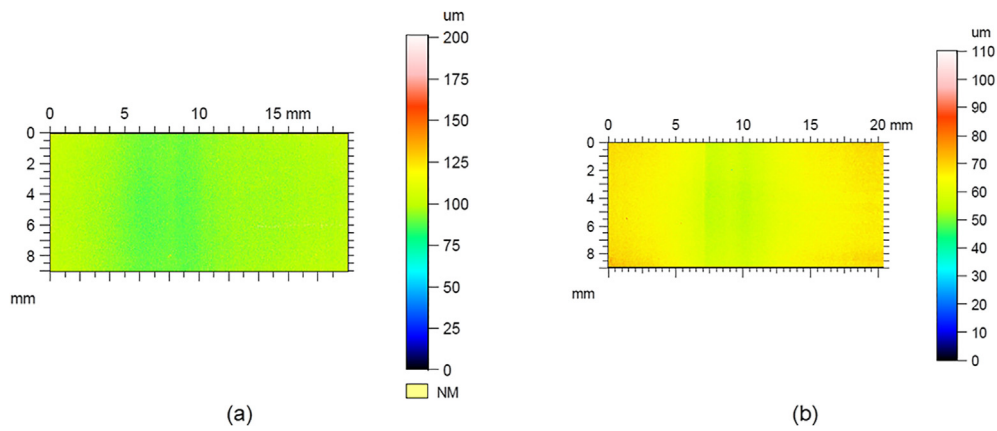
Table 4. Confocal microscope parameters used for 3D roughness measurements.

Roughness instrument			
Objective	10X	Resolution	12μm
Overlap area	10%	Threshold	10%
Z-Scan value	200μm		

Figure 11. 2D surface profile for (a) First contour cut and (b) Second contour cut.

Table 5. Cutting conditions, deformation collection and data analysis parameters for the second "improved" contour measurement.

Case	Cutting wire Diameter (mm)	Deformation spacing, d (mm)	Knot spacing, k (mm)	FE mesh size, s (mm)	Residual stress wavelength, w (mm)
Improved Contour	0.15	0.125	0.4	0.25	3
Criteria	0.25	$<< k, \leq w/12$	$\leq w/4$	$\geq d, \leq w/12$	w
Met	Yes	Yes	Yes	Yes	-

state phase transformation during the weld fusion zone cooling process [54, 55]. The low values of stresses close to the weld center also coincide with the hardness measurement results showed in the previous study that was conducted on the same plate [39], which indicates the extent of the martensitic zone created during cool down. The differences in the location and magnitude of both the tensile stress peaks in the new contour method results and neutron diffraction results are mainly because there are some limitations associated with the comparison of the results of both the techniques. In the studies [44, 49] for the neutron diffraction results,

the lattice parameter variation in the Ferrite BCC-lattice caused only by the residual stresses were considered and any variations due to the chemical composition modifications after the electron-beam welding were not considered. The lattice constant can also be affected by the amount of carbon and the other elements in the BCC-phase. Moreover, both the methods are executed using different gauge sizes. The neutron diffraction measurements were conducted using $(1 \times 1 \times 1)$ mm^3 gauge size. For the contour method it can be argued that the first order finite element mesh size, s, represents the gauge size providing an appropriate
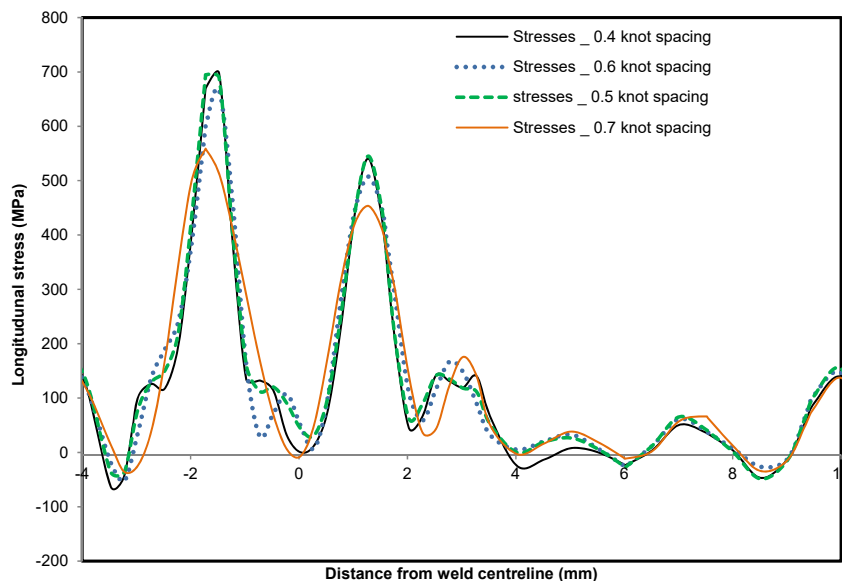

Figure 12. Showing the effect of change in knot spacing for element mesh size (0.25 mm).

knot size has been used with sufficient measurement density. Thus, the new contour measurement had an effective "gauge size" of 0.25 mm and therefore this captured the stress field near to the weld more precisely.

4. Conclusions

The following conclusions can be drawn from the present study.

- The contour method, as conventionally applied, failed to provide a detailed characterisation of the short length scale residual stress distributions that can be formed as a result of advance welding techniques such as high power density electron beam welds
- The criteria developed in [48] by the author, informing choices for contour method data analysis parameters, can be successfully applied to capture short length scale residual stress variations (2–3 mm peak to peak) if the wavelength of such variations can be estimated.
- Contour method measurements can be significantly improved by careful execution of the cutting process, surface measurement steps, and suitable selection of data analysis parameters.
- The quality of the contour cut surfaces can be improved by undertaking following measures.
  - Use of thinner WEDM wire diameters.
  - Careful selection of wire WEDM cutting parameters.
  - Use of sacrificial layers at the both faces (top and bottom) of the plate along the plane of the contour cut, as well as at the start and end of the cut.
  - Use of embedded cutting configuration.
- Improved quality of the contour cut surfaces allows a finer deformation measurement spacing to be used that can help to capture the underlying short length scale surface features.
- In this study, in order to capture the short length scale stress variations fine knot spacings were used. This caused the problem of unrealistic sharp stress variations appearing away from the peak tensile stress region. This is most likely to be because of the over fitting of the surface displacement data away from the weld region. This problem can be resolved by controlling the knot spacing along the cut length. Finer knot spacing can be used for highly concentrated stress region and short residual stress length-scale and for the rest of the cut length relatively coarser knot spacing can be used where the wavelength of this stress field is much larger.

Declarations

Author contribution statement

N. Naveed: Conceived and designed the experiments; Performed the experiments; Analyzed and interpreted the data; Contributed reagents, materials, analysis tools or data; Wrote the paper.

Funding statement

This research did not receive any specific grant from funding agencies in the public, commercial, or not-for-profit sectors.

Data availability statement

Data associated with this study has been deposited at https://sure.sunderland.ac.uk/

Declaration of interests statement

The authors declare no conflict of interest.

Additional information

No additional information is available for this paper.

References

[1] R.L. Klueh, Elevated temperature ferritic and martensitic steels and their application to future nuclear reactors, Int. Mater. Rev. 50 (5) (2005) 287–310.

[2] F. Abe, M. Tabuchi, Microstructure and creep strength of welds in advanced ferritic power plant steels, Sci. Technol. Weld. Join. 9 (1) (2004 Jan) 22–30.

[3] J. Francis, W. Mazur, H. Bhadeshia, Type IV cracking in ferritic power plant steels, Mater. Sci. Technol. 22 (12) (2006) 1387–1395.

[4] K.K. Coleman, W.F. Newell, P91 and beyond, Weld J-N Y. 86 (8) (2007) 29.

[5] M. Tabuchi, T. Watanabe, K. Kubo, M. Matsui, J. Kinugawa, F. Abe, Creep crack growth behavior in the HAZ of weldments of W containing high Cr steel, Int. J. Pres. Ves. Pip. 78 (11–12) (2001 Nov 12) 779–784.

[6] S. Spigarelli, E. Quadrini, Analysis of the creep behaviour of modified P91 (9Cr–1Mo–NbV) welds, Mater. Des. 23 (6) (2002 Sep) 547–552.

[7] S. Paddea, J.A. Francis, A.M. Paradowska, P.J. Bouchard, I.A. Shibli, Residual stress distributions in a P91 steel-pipe girth weld before and after post weld heat treatment, Mater. Sci. Eng. A 534 (2012 Feb) 663–672.

[8] S.K. Albert, M. Tabuchi, H. Hongo, T. Watanabe, K. Kubo, M. Matsui, Effect of welding process and groove angle on type IV cracking behaviour of weld joints of a ferritic steel, Sci. Technol. Weld. Join. 10 (2) (2005) 149–157.

[9] H. Schultz, Electron Beam Welding, Elsevier, 1994, p. 245.

[10] W.H. Giedt, L.N. Tallerico, Prediction of electron beam depth of penetration, Weld. J. 67 (12) (1988) 299–305.

[11] J.F. Lancaster, Handbook of Structural Welding: Processes, Materials and Methods Used in the Welding of Major Structures, Pipelines and Process Plant, Elsevier, 1997, p. 445.

[12] B. Joseph, D. Katherasan, P. Sathiya, C.S. Murthy, Weld metal characterization of 316L (N) austenitic stainless steel by electron beam welding process, Int. J. Eng. Sci. Technol. 4 (2) (2012) 169–176.

[13] C. Liu, B. Wu, J.X. Zhang, Numerical investigation of residual stress in thick titanium alloy plate joined with electron beam welding, Metall. Mater. Trans. B 41 (5) (2010) 1129–1138.

[14] H.J. Stone, P.J. Withers, S.M. Roberts, R.C. Reed, T.M. Holden, Comparison of three different techniques for measuring the residual stresses in an electron beam-welded plate of WASPALOY, Metall. Mater. Trans. 30 (7) (1999) 1797–1808.

[15] G. Zheng, D. Smith, A new procedure for measuring residual stresses in electron beam welds using the deep hole drilling technique, in: The Society for Experimental Mechanics Series 2011, 2011, pp. 75–84.

[16] F. Hosseinzadeh, A.H. Mahmoudi, C.E. Truman, D.J. Smith, Prediction and measurement of through thickness residual stresses in large quenched components, in: Proceedings of the World congress on Engineering, Citeseer, 2009.

[17] P.K. Taraphdar, J.G. Thakare, C. Pandey, M.M. Mahapatra, Novel residual stress measurement technique to evaluate through thickness residual stress fields, Mater. Lett. 277 (2020 Oct 15) 128347.

[18] M.E. Fitzpatrick, A. Lodini, Analysis of Residual Stress by Diffraction Using Neutron and Synchrotron Radiation, CRC Press, 2003, p. 367.

[19] P.J. Withers, M. Preuss, A. Steuwer, J.W.L. Pang, Methods for obtaining the strain-free lattice parameter when using diffraction to determine residual stress, J. Appl. Crystallogr. 40 (5) (2007 Oct 1) 891–904.

[20] D.W. Brown, T.M. Holden, B. Clausen, M.B. Prime, T.A. Sisneros, H. Swenson, et al., Critical comparison of two independent measurements of residual stress in an electron-beam welded uranium cylinder: neutron diffraction and the contour method, Acta Mater. 59 (3) (2011) 864–873.

[21] M.B. Prime, Cross-sectional mapping of residual stresses by measuring the surface contour after a cut, J. Eng. Mater. Technol. 123 (2) (2000 Nov 3) 162–168.

[22] M. Prime, A.T. DeWald, The contour method, in: Practical Residual Stress Measurement Methods, John Wiley & Sons, Ltd, 2013, pp. 109–138.

[23] M. Prime, M. Hill, A. DeWald, R. Sebring, V. Dave, M. Cola, Residual stress mapping in welds using the contour method, in: The 6th International Conference. Pine Mountain, ASM International, Georgia, 2002, pp. 891–896.

[24] Y. Traore, S. Paddea, P.J. Bouchard, M.A. Gharghouri, Measurement of the residual stress tensor in a compact tension weld specimen, Exp. Mech. 53 (4) (2013) 605–618.

[25] F. Hosseinzadeh, M.B. Toparli, P.J. Bouchard, Slitting and contour method residual stress measurements in an edge welded beam, J. Pressure Vessel Technol. 134 (1) (2012) 11402–11406.

[26] A.T. DeWald, M.R. Hill, Eigenstrain-based model for prediction of laser peening residual stresses in arbitrary three-dimensional bodies Part 1: model description, J. Strain Anal. Eng. Des. 44 (1) (2009 Jan 1) 1–11.

[27] A. Evans, G. Johnson, A. King, P.J. Withers, Characterization of laser peening residual stresses in Al 7075 by synchrotron diffraction and the contour method, J. Neutron Res. 15 (2) (2007 Jun) 147–154.

[28] Y. Zhang, S. Ganguly, V. Stelmukh, M.E. Fitzpatrick, L. Edwards, Validation of the contour method of residual stress measurement in a MIG 2024 weld by neutron and synchrotron X-ray diffraction, J. Neutron Res. 11 (4) (2003 Dec) 181–185.

[29] V. Richter-Trummer, S.M. Tavares, P.M. Moreira, M.A. de Figueiredo, P.M. de Castro, Residual stress measurement using the contour and the sectioning methods in a MIG weld: effects on the stress intensity factor, Ciênc. Tecnol. Mater. 20 (1–2) (2008) 114–119.

[30] M.B. Prime, T. Gnäupel-Herold, J.A. Baumann, R.J. Lederich, D.M. Bowden, R.J. Sebring, Residual stress measurements in a thick, dissimilar aluminum alloy friction stir weld, Acta Mater. 54 (15) (2006 Sep) 4013–4021.

[31] P. Frankel, M. Preuss, A. Steuwer, P.J. Withers, S. Bray, Comparison of residual stresses in Ti–6Al–4V and Ti–6Al–2Sn–4Zr–2Mo linear friction welds, Mater. Sci. Technol. 25 (5) (2009) 640–650.

[32] M. Turski, L. Edwards, Residual stress measurement of a 316L stainless steel bead-on-plate specimen utilising the contour method, Int. J. Pres. Ves. Pip. 86 (1) (2009) 126–131.

[33] L. Hacini, N.V. Lê, P. Bocher, Evaluation of residual stresses induced by robotized hammer peening by the contour method, Exp. Mech. 49 (6) (2008 Dec 16) 775–783.

[34] A.T. DeWald, J.E. Rankin, M.R. Hill, M.J. Lee, H.-L. Chen, Assessment of tensile residual stress mitigation in Alloy 22 welds due to laser peening, J. Eng. Mater. Technol. 126 (4) (2004) 465–473.

[35] O. Hatamleh, J. Lyons, R. Forman, Laser peening and shot peening effects on fatigue life and surface roughness of friction stir welded 7075-T7351 aluminum, Fatig. Fract. Eng. Mater. Struct. 30 (2) (2007) 115–130.

[36] O. Hatamleh, Effects of peening on mechanical properties in friction stir welded 2195 aluminum alloy joints, Mater. Sci. Eng. A 492 (1) (2008) 168–176.

[37] Y. Zhang, M.E. Fitzpatrick, L. Edwards, Measurement of the residual stresses around a cold expanded hole in an EN8 steel plate using the contour method, in: Materials Science Forum, Trans Tech Publ, 2002, pp. 527–534.

[38] M.B. Prime, M.A. Newborn, J.A. Balog, Quenching and cold-work residual stresses in aluminum hand forgings: contour method measurement and FEM prediction, Mater. Sci. Forum 426–432 (2003) 435–440.

[39] A. Kundu, P.J. Bouchard, S. Kumar, K.A. Venkata, J.A. Francis, A. Paradowska, et al., Residual stresses in P91 steel electron beam welds, Sci. Technol. Weld. Join. 18 (1) (2013 Jan) 70–75.

[40] W. Rae, Z. Lomas, M. Jackson, S. Rahimi, Measurements of residual stress and microstructural evolution in electron beam welded Ti-6Al-4V using multiple techniques, Mater. Char. 132 (2017 Oct 1) 10–19.

[41] M.B. Prime, System and Method for Measuring Residual Stress. United States: Los Alamos National Laboratory (LANL), Los Alamos, NM, 2002. Report No.: US 6470756.

[42] M.B. Prime, A.L. Kastengren, The contour method cutting assumption: error minimization and correction, in: Experimental and Applied Mechanics 6, Springer, 2011, pp. 233–250.

[43] Y. Traore, Controlling plasticity in the contour method of residual stress measurement (PhD thesis), in: Materials Science & Engineering, The Open University, 2013.

[44] M.D. Olson, A.T. DeWald, M.B. Prime, M.R. Hill, Estimation of uncertainty for contour method residual stress measurements, Exp. Mech. 1–9 (2014).

[45] F. Hosseinzadeh, P. Ledgard, P.J. Bouchard, Controlling the cut in contour residual stress measurements of electron beam welded Ti-6Al-4V alloy plates, Exp. Mech. 53 (5) (2013) 829–839.

[46] P.J. Bouchard, P. Ledgard, S. Hiller, F. Hosseinzadh Torknezhad, Making the Cut for the Contour Method, 2012. Porto, Portugal.

[47] F. Hosseinzadeh, N. Naveed, Residual Stress Measurement in Three Pass Groove Welded Plate Using the Contour Method, The Open University, Milton Keynes, UK, 2013. Report No.: OU/MatsEng/042, Issue 1.

[48] N. Naveed, Guidelines to select suitable parameters for contour method stress measurements, Arch. Mech. 72 (1) (2020 Feb 27) 39–58–58.

[49] A. Kundu, P.J. Bouchard, S. Kumar, G.K. Dey, Characterisation of residual stress in electron beam welded P91 plates by neutron diffraction, Int. J. Metall. Eng. 2 (1) (2013) 79–84.

[50] M.B. Prime, R.J. Sebring, J.M. Edwards, D.J. Hughes, P.J. Webster, Laser surface-contouring and spline data-smoothing for residual stress measurement, Exp. Mech. 44 (2) (2004 Apr 1) 176–184.

[51] F. Hosseinzadeh, J. Kowal, P.J. Bouchard, Towards good practice guidelines for the contour method of residual stress measurement, J. Eng. (2014). Online-only.

[52] M. Prime, A. Kastengren, The contour method cutting assumption: error minimization and correction, in: Conference Proceedings of the Society for Experimental Mechanics Series, 2011, pp. 233–250.

[53] Y.L. Sun, M.J. Roy, A.N. Vasileiou, M.C. Smith, J.A. Francis, F. Hosseinzadeh, Evaluation of errors associated with cutting-induced plasticity in residual stress measurements using the contour method, Exp. Mech. 57 (5) (2017 Jun) 719–734.

[54] J.A. Francis, M. Turski, P.J. Withers, Measured residual stress distributions for low and high heat input single weld beads deposited on to SA508 steel, Mater. Sci. Technol. 25 (3) (2009) 325–334.

[55] H. Dai, J.A. Francis, P.J. Withers, Prediction of residual stress distributions for single weld beads deposited on to SA508 steel including phase transformation effects, Mater. Sci. Technol. 26 (8) (2010) 940–949.